GOCE QUICK-LOOK GRAVITY FIELD ANALYSIS IN THE FRAMEWORK OF HPF

Roland Pail[(1)], Bernhard Metzler[(1)], Thomas Preimesberger [(1)], Barbara Lackner [(1)], Martin Wermuth [(2)]

[(1)] Graz University of Technology, Institute of Navigation and Satellite Geodesy, Steyrergasse 30, 8010 Graz, Email: pail@geomatics.tu-graz.ac.at
[(2)] Technical University Munich, Institute of Astronomical and Physical Geodesy, Arcisstraße 21, 80333 Munich, Email: wermuth@bv.tu-muenchen.de

ABSTRACT

The Quick-Look Gravity Field Analysis (QL-GFA) is a component of the Routine & Rapid Processing Facilities in the framework of the ESA-funded project "GOCE High-level Processing Facility" (HPF), an operational hardware and software system for the scientific processing (Level 1b to Level 2) of GOCE data. The purpose of the QL-GFA is to analyze partial and/or incomplete sets of gravity gradient and orbit data, in order to derive a fast diagnosis of the GOCE system performance in parallel to the mission, and thus to provide a fast feedback to GOCE mission control. Key products are quick-look gravity field models and estimates of the gradiometer error PSD. The paper gives an overview of the operational QL-GFA software system. On the basis of a numerical case study, which is based on the data of an ESA GOCE end-to-end simulation, the key components of the QL-GFA processing architecture are addressed, and the information content of all relevant output products is presented and discussed.

1. INTRODUCTION

The scientific GOCE data processing (Level 1b to Level 2) is performed by the "European GOCE Gravity Consortium" (EGG-C), a consortium of 10 European university and research institutes, in the framework of the ESA-funded project "GOCE High-Level Processing Facility" (HPF; [16]). In addition to the production of precise GOCE orbits, calibrated gravity gradients and a high-accuracy, high-resolution GOCE spherical harmonic model of the Earth's gravity field including variance-covariance information (in a post-processing step), one component of HPF deals with the generation of quick-look products (rapid science orbits, approximate gravity field models) already in parallel to the GOCE measurement phases. The main purpose of these quick-look products is to derive a fast diagnosis of the GOCE sensor systems, and thus to contribute to ESA's calibration and validation activities. In the frame of this HPF contract, the "Sub-processing Facility (SPF) 6000", a co-operation of TU Graz, Austrian Academy of Sciences, University of Bonn, and TU Munich, under the lead of TU Graz, is – in addition to the production of a high-precision GOCE gravity field model – also responsible for the processing of quick-look gravity field models from preliminary GOCE orbit data applying satellite-to-satellite tracking in the high-low mode (hl-SST), and satellite gravity gradiometry (SGG).

2. KEY TASKS OF QL-GFA

Key tasks of QL-GFA are:

- Check of SGG and hl-SST input data in parallel to the mission and analysis of partial / incomplete SGG and hl-SST data sets.
- Computation of quick-look gravity field models (SST-only, SGG-only, combined SST+SGG) for the purpose of a fast analysis of the information content of the input data on the level of the gravity field solution.
- Estimation of the gradiometer error PSD (power spectral density) from the residuals of a SGG-only gravity field analysis, and application of previously defined statistical hypothesis test strategies in time and frequency domain. Therefore, the question whether the a priori gradiometer error model is realistic can be answered, and optimal filters for an ultimate-precision adjustment can be designed.
- Production of Quality Report Sheets: All these system diagnosis products will be accompanied with a proper error description and related statistical confidence levels. The system diagnosis will be reported by means of a standardized Quality Report Sheet.

QL-GFA will be applied at two stages: Quick-Look-A (QL-A) is applied to Level 1b preliminary orbits (accuracy ~10 m) and the Level 1b gravity gradients. The main purpose at this stage is a rough check of the SGG measurement time series, with special emphasis on the testing of the SGG error PSD. For QL-A, consecutive gravity field solutions will be available in a daily interval. They will be generated with a latency of 4 hours after arrival of all required input data. The achievable accuracy is mainly dependent on the correct (internal) calibration of the Level 1b gradients.

Proc. 'The 3rd International GOCE User Workshop', ESA-ESRIN, Frascati, Italy, 6–8 November 2006 (ESA SP-627, January 2007)

Quick-Look-B (QL-B) is applied after the availability of the Level 2 rapid science orbit solution (accuracy in the decimetre range) and the calibrated gravity gradients. In this phase, the corresponding SST and SGG time series are checked on the level of the Earth's gravity field, also testing the gradiometer error model. For QL-B, consecutive gravity field solutions will be available in a weekly interval. The maximum degree and order for the QL-GFA gravity field models will be optimized with respect to the global coverage of the input data.

3. FUNCTIONAL MODEL

The QL-GFA is based on the semi-analytic approach. While in the direct and space-wise solution strategies, the observations are regarded as functions of the geographical location (r,ϑ,λ), they can also be considered as a periodic time-series for one repeat period ([15]). Assuming a circular orbit, the gravitational potential V and also derived gravity functionals $V^{(\kappa)}$ can be rewritten as a Fourier series

$$V^{(\kappa)}(t) = \sum_m \sum_k \left[A_{km}^{(\kappa)} \cos\psi_{km}(t) + B_{km}^{(\kappa)} \sin\psi_{km}(t) \right] \quad (1)$$

where $\psi_{km}(t)$ is related to the two fundamental frequencies ω_o (satellite orbit revolution) and ω_e (Earth's rotation). The spherical harmonic coefficients C_{lm}, S_{lm} of the same order m are lumped together in a linear way to compose the Fourier coefficients $A_{lm}^{(\kappa)}$ and $B_{lm}^{(\kappa)}$ ([15]), leading to a block-diagonal structure of the corresponding normal equation matrix.

QL-GFA solutions complete to degree/order 250 can be processed within the order of one to two hours on a standard PC. The efficiency and speed of QL-GFA is founded mainly on the application of FFT techniques, a simplified filter strategy in the spectral domain to cope with the coloured noise characteristics of the gradiometer, and the assumption of block-diagonality of the normal equation matrix. Deviations from this assumption are incorporated by means of an iterative procedure.

A detailed discussion of the theory and the mathematical models of the QL-GFA software can be found in [9]. The QL-GFA method was already successfully applied in the framework of realistic GOCE closed-loop simulations ([11], [12]), also in the case of short data sets, data gaps and non-closing orbits ([9], [13]), [14]).

4. SOFTWARE ARCHITECTURE

Fig. 1 shows the architectural design, the main components and the product flow through the QL-GFA software system.

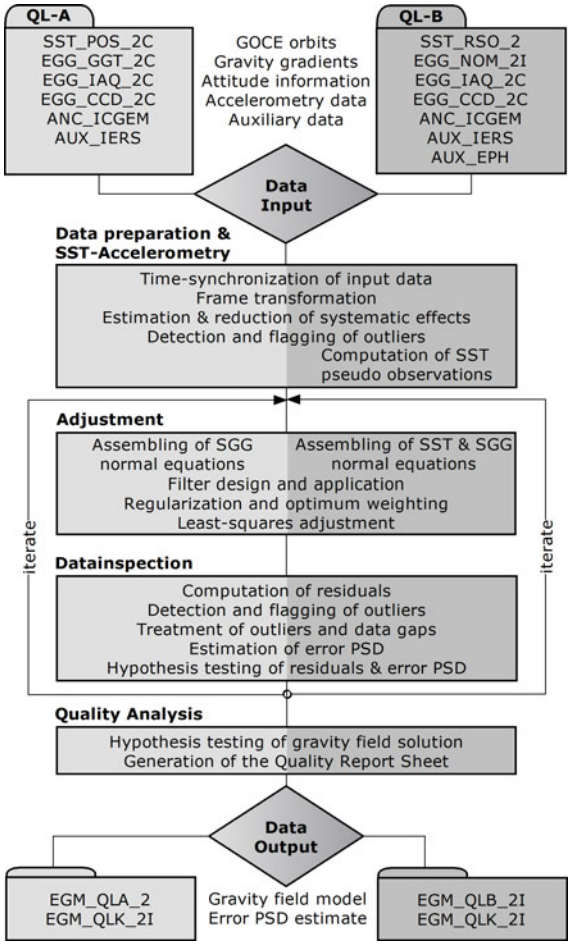

Fig. 1. QL-GFA: Architectural design and product flow

In the following, the main modules shall be briefly described. Selected features of the QL-GFA processing will be addressed in chapter 5.

Input:
In the case of QL-A processing, exclusively Level 1b data and some auxiliary data products are used. In this software mode, the start of the processing is fully automated. It is checked in regular intervals whether new data have arrived via the official HPF interface, the processing is started and operated automatedly until the delivery of the QL-GFA output products again via the official interface.
In the case of QL-B processing, a mixture of Level 1b data (e.g., attitude information, accelerometry data), Level 2 data (rapid science orbits, preliminary externally calibrated gradients) and auxiliary products is used.

Data Preparation and SST-Accelerometry:
During this pre-processing phase, orbit and gradiometry data are time-synchronized, and the transformation among different reference frames (gradiometer reference frame (GRF), inertial frame, Earth-fixed frame) is computed. Potentially occurring systematic

and extreme long-periodic effects in the SGG measurement time series are estimated and reduced (cf. section 5.1), and outlier detection strategies are applied to the input time series (cf. section 5.2). The SST processing is based on the energy integral approach ([1], [2]). Therefore, in the case of the processing of SST-only or combined SST+SGG solutions, the SST pseudo-observations are computed, including the correct treatment of non-conservative forces and tidal effects.

Adjustment:
The normal equations are assembled applying the functional model described in chapter 3. As filter information, representing the metrics of the system, either an a-priori noise model, or alternatively the error PSD estimates derived in the previous iteration are used. The normal equation systems are superposed, applying optimum weights for the individual SGG components V_{XX}, V_{YY} and V_{ZZ}, and the SST component. These weights are derived by variance-component estimation. Finally, the coefficients are computed by a block-wise least squares adjustment, where, optionally, regularization is applied (cf. section 5.3).

Data Inspection:
The residuals related to the coefficient estimates are computed and checked for outliers. Based on the cleaned SGG residuals, the gradiometer error PSD is estimated, which can be used as filter information in the subsequent iteration. Finally, hypothesis test strategies in time and frequency domain are applied to the residuals, in order to check them against an a-priori gradiometer error model (cf. section 5.4).

Quality Analysis:
After finalization of the iterative procedure, as a validation procedure also the final gravity field solution is statistically checked against an a-priori model (cf. section 5.5). Finally, a Quality Report Sheet, which summarizes the results of the statistical tests, is generated.

Output:
Table 1 gives an overview of the official output products. Additionally, several internal products (residuals, flags, regularization and weighting parameters) are generated.

Table 1: Output products of QL-GFA

Identifier	Product description
EGM_QLA_2	QL gravity field solution from SGG-only, based on Level 1b data
EGM_QLB_2i EGM_QST_2i EGM_QSG_2i EGM_QCO_2i EGM_QQR_2i	QL solutions based on Level 2 data: SST-only gravity field model SGG-only gravity field model combined SST+SGG grav. model Quality Report Sheet
EGM_QLK_2i	GOCE error PSD estimate

These products are also used as prior information for the Core Solver processing, i.e., the processing of a high-accuracy GOCE Earth's gravity field model and the corresponding full variance-covariance matrix, which is the second main task of SPF 6000 ([10]).

5. SELECTED FEATURES OF QL-GFA

5.1 Estimation of systematic effects

The 1/f-characteristics of the SGG noise spectrum below the gradiometer measurement bandwidth (Fig. 3) can lead to extremely long-wavelength and systematic errors with a very high amplitude. In the semi-analytic approach it is extremely difficult to co-estimate additional parameters. Therefore, selected parameters which shall absorb the systematic signal content are adjusted together with a reduced set of gravity field parameters in a pre-processing step. From these systematic parameters, a reduction time series is computed, which is subtracted from the SGG measurement time series before the actual quick-look gravity field processing.

Let us assume that gravity gradients are available for a certain time period Γ. For the parameterization of systematic effects, this total period is split into $k = 1, \ldots K$ parts of length T_k. Thus, the starting epoch of each section is t_k^o, and the last epoch is t_k^e. For each part k, the additional parameter model for the systematic effects is a linear combination of Legendre polynomials, and reads:

$$f_k(t) = \sum_{n=0}^{N} P_n(\tau)\, a_n \;;\; t \in [t_k^o, t_k^e] \qquad (2)$$

with the base functions (Legendre polynomials) P_n of maximum degree N, and a_n denoting the corresponding coefficients. The argument τ is a mapping of the original time t, so that: $t \in [t_k^o, t_k^e] \rightarrow \tau \in [-1, 1]$. This time transformation guarantees that the base functions P_n are defined on their natural definition domain. Although they are not strictly orthogonal when applied to an equi-distantly sampled discrete time series, this choice of the additional parameter model guarantees well-conditioned normal equation systems. Since systematic effects turn out to be mainly correlated with the zonal harmonic coefficients, they are estimated together with the systematic parameters, yielding the observation equations for the gravity gradient component *[c]*, which can hold *[c]* = V_{XX}, V_{YY} or V_{ZZ}:

$$y^{[c]} + v^{[c]} = A^{[c]}\, x = \sum_{l=0}^{L} \overline{P}_{l0}\; \overline{C}_{l0} + \sum_{k=1}^{K} \left(\sum_{n=0}^{N} P_n^{(k)}(\tau)\, a_n^{(k)} \right)^{[c]} \qquad (3)$$

While the (gravity) base functions $\overline{P}_{l0}$ are valid for the total period Γ and are set-up as a sum of all three components *[c]*, the (systematic) base functions P_n^k are only defined within their respective time interval *k*, individually for each component *[c]*. Based on this observation model, a rigorous least squares adjustment is performed to solve for the parameters $x = \{\overline{C}_{l0}; a_n^{(k)}\}$. The systematic effect models are assumed to be uncorrelated among the components *[c]*.

In order to avoid discontinuities of the systematic reduction time series at the splitting epochs, additional conditions are introduced, requiring that the function representing the systematic effect is continuously differentiable everywhere, i.e., also at the splitting epochs. The corresponding conditions read

$$\begin{aligned} f_k(t_k^e) &= f_k(t_{k+1}^o) \\ f_k^{/}(t_k^e) &= f_k^{/}(t_{k+1}^o) \end{aligned} \qquad (4)$$

and can be co-adjusted applying a standard parameter adjustment with additional conditions. The frequency content of the systematic effects can be influenced by the choice of the maximum *L* in combination with the number of parts *K*.

5.2 Outlier detection

For the detection of outliers, a combination of

- an outlier detection method based on wavelets,
- a variant of the Dixon test, and
- a thresholding method

is used. A numerical assessment of these (and other) methods can be found in ([3]).

The outlier detection cannot only be applied in pre-processing, but a considerably improved performance can be achieved when applying it also to the residuals of the gravity field adjustment (after every iteration of the QL-GFA). This gain in performance is due to the increased noise-to-signal ratio. In the QL-GFA implementation, the wavelet method and the Dixon test are applied a priori, while the Dixon test and the thresholding method are applied successively to the residuals after each iteration.

5.3 Regularization

As the baseline regularization strategy, the Spherical Cap Regularization Approach (SCRA) is applied ([7]). This regularization technique is dedicated to the specific problem of the non-polar orbit configuration of the GOCE satellite. The main idea of the SCRA is the filling of the polar gaps, where no GOCE observations are available, with an artificial signal, which shall be described analytically. The main advantage of this method is that it is spatially restricted to the problem areas of the polar gaps. Unlike standard regularization techniques, such as Kaula or Tikhonov regularization, which act on the parameters to be estimated in spectral domain (harmonic coefficients), the SCRA acts almost purely in space domain, and thus represents an optimum strategy for the reduction of the polar gap problem.

5.4 Hypothesis tests on residuals and PSD estimates

A software module containing statistical hypothesis test methods in frequency and in time domain, applicable also to very long data sets, has been set-up ([5]). The individual tests are arranged in a continuous test sequence, which guarantees the fulfilment of necessary assumptions. These tests shall check the consistency of the SGG measurement time series, and test the PSD estimates calculated from the residuals of the adjustment against an a-priori GOCE error PSD.

5.5 Statistical validation of gravity field products

The gravity field solutions are internally validated by means of independent global gravity field models, applying hypothesis test strategies ([9]).

It is assumed that the following information is available:
1. QL-GFA gravity field solution represented by spherical harmonic coefficients $\hat{x} = \{\overline{C}_{lm}, \overline{S}_{lm}\}$, including an associated statistical error information in terms of a variance-covariance matrix $\Sigma(\hat{x})$. In the case of QL-GFA, this is a block-diagonal matrix, because only the coefficients of a certain order m are correlated.
2. A priori gravity field model $x^{(o)} = \{\overline{C}_{lm}^{(o)}, \overline{S}_{lm}^{(o)}\}$, including variance- covariance information $\Sigma(x^{(o)})$, which should be *independent* of the QL-GFA solution.

Starting from these input quantities, a random vector *x* is defined as the difference between the estimated coefficients $\hat{x}$ and the reference coefficients $x^{(o)}$: $x = \hat{x} - x^{(o)}$. The corresponding variance-covariance matrix can be derived by applying covariance propagation: $\Sigma(x) = \Sigma(\hat{x}) + \Sigma(x^{(o)})$. The fact that there is no mixed term $\Sigma(\hat{x}, x^{(o)})$ is strictly valid, because of the assumption of independent models.

The null hypothesis H_0 is given as

$$H_0 : x_i = 0_{(q-p+1,1)}, \forall i \in \{p, p+1, ..., q\} \qquad (5)$$

versus the alternative hypothesis H_1 that there exists at least one *i* for which $x_i \neq 0$. Here, *p* and *q* are arbitrary

indices of the parameter vector x of length s, with $p \le q \le s$, defining a sub-set of parameters.

If the null hypothesis is true, the test statistic T follows ([4]):

$$T = \frac{1}{q-p+1} x_{p...q}^T \cdot \Sigma(x)_{p...q}^{-1} \cdot x_{p...q} \qquad (6)$$

The test variable T is Fisher-F-distributed at a level of significance $T = F_{1-\alpha}(q-p+1, n-s)$, where n is the number of the observations the random vector x is based on, which is usually very large: $(n\text{-}s) \to \infty$.

In principle, the indices p and q can be chosen arbitrarily. In the special case of the GOCE gravity field models, several strategies for the partitioning of x and correspondingly of $\Sigma(x)$ can be favoured:

- Case: $p = q = i$: In this case, Eq. (6) is evaluated separately for each coefficient $\overline{C}_{lm}, \overline{S}_{lm}$, respectively, leading to a full spectral triangle $T_{lm} = \{T_{lm}^{(c)}, T_{lm}^{(s)}\}$ of test variables.
- Case: Partitioning into blocks for each order m separately, leading to m-dependent test variables T_m. This strategy is driven by the block-diagonal structure of the QL-GFA normal equations.
- Case: $p = 1$, $q = s$: Simultaneous analysis of all coefficients, taking the full covariances into account. This leads to a scalar test variable T.

A special case of this hypothesis test strategy can be applied in a closed-loop simulation, where the reference gravity field model is a-priori known, and thus the variance-covariance matrix of the reference model yields $\Sigma(x^{(o)}) = 0$. In this special case, the absolute coefficient errors x, i.e. deviations from the true model, are compared with the corresponding error estimates $\Sigma(x)$, and thus simply the consistency of the error behaviour of the coefficient estimate and the corresponding statistical error estimate is checked. It should be emphasized, that such a modified test configuration is theoretically correct, because in this case the requirement of an independent reference model is no longer necessary.

6. NUMERICAL CASE STUDY

6.1 Test data sets

The numerical case study is based on the data of an ESA GOCE end-to-end simulation. This test configuration was also used during the official Acceptance Review 2 for the testing of the final operational software (at the end of the development phase) in the framework of the HPF. The test data sets consist of:

- *Gravity gradients*: 25 days of 1 Hz rate simulated gravity gradients defined in the Gradiometer Reference Frame, based on the gravity field model EGM96 ([6]) complete to degree/order 360, superimposed by colored noise (cf. Fig. 3).
- *Orbit*: The gradients are defined along an orbit with GOCE characteristics (inclination i = 96.5°, eccentricity $e < 2 \cdot 10^{-3}$, mean altitude ~240 km). The orbit positions (and velocities) were generated by orbit integration, based on the gravity model EGM96, complete to degree/order 200, and including a full external force model and drag free and attitude control (DFAC) simulation. The orbit velocities were superposed by white noise with a standard deviation of 0.1 mm/s.
- *Attitude*: The orientation of the satellite body axes (and hence the GRF) with respect to the inertial frame is given in terms of quaternions. These quaternions are computed from a combination of star tracker and gradiometer information. Correspondingly, they include attitude biases and noise ([8]), related to the star tracker and gradiometer inaccuracies modelled in the end-to-end simulation.

Due to the fact that a "partial data set" of only 25 days of data is processed, the maximum degree of resolution of the parameter model was chosen as 200. Therefore, a small spectral leakage effect is expected to occur in the results. Since signals up to degree/order 360 are inherent in the measurement time series, these high-frequency contributions (degree/order 201 to 360) are leaking into the spectral range covered by the parameter model.

6.2 Results: QL-A

As mentioned in chapter 2, QL-A is applied to Level 1b preliminary orbits (with an accuracy in the order of 10 to 20 m), and to Level 1b gravity gradients. Main output products are a SGG-only gravity field solution, and a first estimate of the SGG error PSDs, complemented by a quality report. The start of the processing and the operation are fully automated.

EGM_QLA_2:

The first main product EGM_QLA_2 contains the spherical harmonic coefficients of the SGG-only solution, as well as a gravity field report. The [green] dotted line in Fig. 4 shows the gravity field solution in terms of the degree error median

$$\sigma_l = median_m \left\{ \left| \overline{R}_{lm}^{(est)} - \overline{R}_{lm}^{(EGM)} \right| \right\} \qquad (7)$$

where $\{\bar{R}_{lm} = \bar{C}_{lm}; \bar{S}_{lm}\}$ are the fully normalized spherical harmonic coefficients, *(est)* denotes the estimated quantities, and *(EGM)* refers to the reference model EGM96.

It clearly shows the very large errors in the low-degree range, which are mainly due to the extreme 1/f characteristics of the SGG noise (Fig. 3), which makes the system very unstable in the low degrees. Therefore, spherical cap regularization was applied to stabilize the system. However, in order to avoid that too much of prior information is introduced – the goal of this processing is the checking of the GOCE system, and therefore a GOCE-only solution is favoured – only the GRS80 normal potential is introduced as stabilizing function in the polar regions $|\varphi| \geq 83.5°$. The weakness of this SGG-only solution in the low degrees can also be observed in the cumulative gravity anomaly errors at degree 200 (cf. Fig. 2). The standard deviation of this field, evaluated in the latitudinal range of $|\varphi| < 83.5°$, which is covered by GOCE observations, is 4.36 mGal.

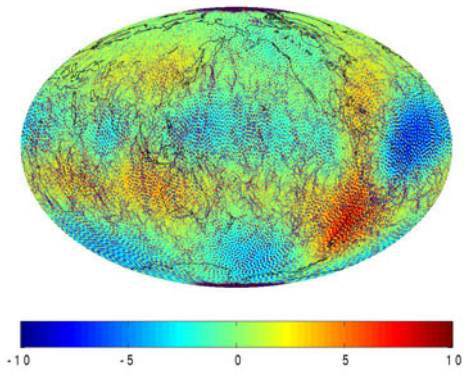

Fig. 2. Cumulative gravity anomaly errors [mGal] at degree 200, based on the QL-A SGG-only solution

EGM_QLK_2i (first version):

Fig. 3 shows the error PSD estimate for the V_{XX} component, computed from the residuals after the final iteration of the gravity field processing. While the black curve shows the (smoothed) 'true' error PSD, the PSD estimate is displayed as [red] dotted curve. Evidently, there are two major deviations of the estimated from the true PSD. First, the error level in the measurement bandwidth of the gradiometer (5 – 100 mHz) is slightly higher. A detailed analysis of this phenomenon reveals, that this is an effect of the inaccurate orbit (~20 m standard deviation), which is additionally affected by data gaps. Second, the peak occurring at a frequency of about 0.04 Hz is an indication of the spectral leakage problem, because this specific frequency can be directly linked to the cut-off degree/order 200 of the parameter model. Similar results are obtained for the components V_{YY} and V_{ZZ} (not shown).

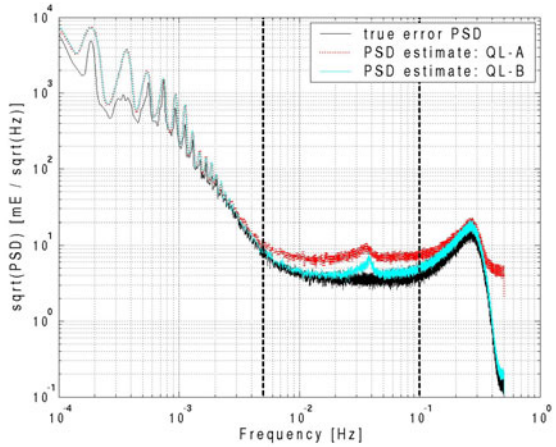

Fig. 3. Estimation of the gradiometer error for the V_{XX} component, based on SGG-only solution. Measurement bandwidth (dashed): 5 – 100 mHz

6.3 Results: QL-B

In the QL-B operation mode, QL-GFA is applied to Level 2 rapid science orbits (with an accuracy in the decimetre range) and Level 2 preliminary calibrated gravity gradients.

EGM_QLB_2i:

QL-B solutions are processed for the configurations:

- SST-only (EGM_QST_2i)
- SGG-only (EGM_QSG_2i)
- Combined solution (EGM_QCO_2i)

Fig. 4 shows the results of these three solutions in terms of the degree error median. Evidently, the combined solution (dashed [blue] curve) is stabilized in the low-degree range mainly by the SST component (light [blue] curve), and dominated by SGG (solid [red] curve) from about degree 20 onwards.

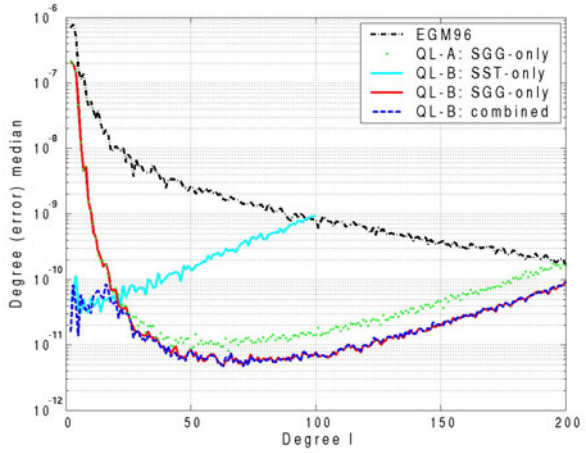

Fig. 4. Degree error medians of QL-A and QL-B gravity field solutions

Also in this case, for the SGG-only and the combined solutions, a weak spherical cap regularization using GRS80 as stabilizing function was applied, and the normal equation systems of the three SGG components and the SST component have been optimally weighted by means of their variance components. In order to demonstrate the stabilization of the combined solution by SST in the low degree region more clearly, Fig. 5 shows the coefficients deviations (left) and the statistical error estimates (right) of the SGG-only (top) and the combined (bottom) solution. The error estimates displayed in Fig. 5 are mean square errors (MSE), i.e., the regularization bias is appropriately accounted for.

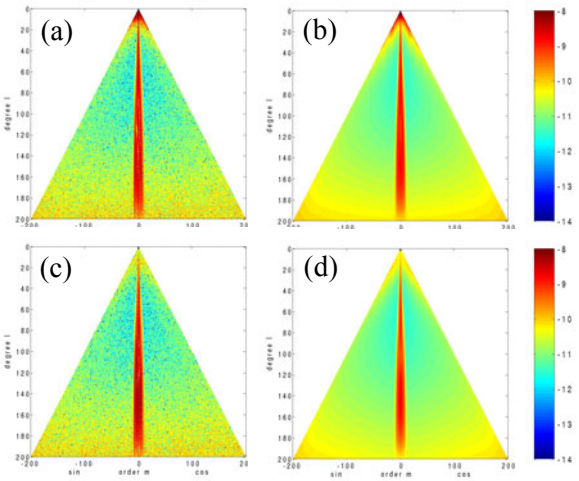

Fig. 5. (a) Coefficient deviations from EGM96 and (b) MSE estimates of the QL-B SGG-only solution; (c) coefficient deviations and (d) MSE estimates of the QL-B combined solution. Scaled in $\log_{10}(|\ldots|)$

The stabilizing effect of the SST-component can also be observed in the cumulative gravity anomaly errors at degree 200, as shown in Fig. 6. The standard deviation of this field in the latitudinal range of $|\varphi| < 83.5°$ is $\sigma_{\Delta g} = 1.78$ mGal, and of a corresponding geoid height difference field $\sigma_N = 6.37$ cm. Taking into consideration that only 25 days of data have been used for this simulation, these results are very satisfactory.

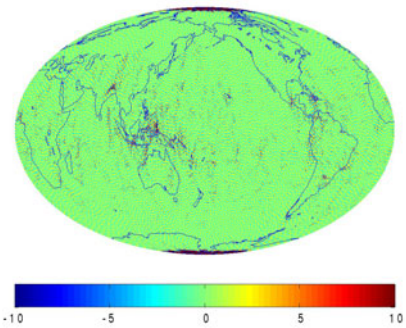

Fig. 6. Cumulative gravity anomaly errors [mGal] at degree 200, based on the QL-B combined solution

EGM_QLK_2i (final version):

The light [blue] curve in Fig. 3 shows the PSD estimate for the V_{XX} component, computed from the residuals of the SGG-only analysis (which does not contain SST information and thus reflects mainly the gradiometer error behaviour). Compared to the first version (dotted [red] curve), the estimate has considerably improved in the measurement bandwidth, which is due to the improved accuracy of the input data (mainly concerning the orbits), and the only remaining significant deviation from the "true" error PSD is the peak due to spectral leakage. In practice, this effect can be reduced by using longer input data sets, enabling the choice of a higher maximum degree of parameterization due to improved ground coverage.

Quality analysis:

The gravity field solutions were also subject to an internal quality assessment, by comparing them statistically with external gravity field models, as described in section 5.5. In this analysis, the hypothesis test was computed for the strict scenario that the reference model, which is the true gravity field model EGM96, is noise-free: $\Sigma(x^{(0)}) = 0$. As explained in section 5.5, such a configuration can only be justified in a numerical case study, where the reference model is perfectly known.

Fig. 7 (a) shows the statistical test variables T_{lm}, when applying the hypothesis tests to the individual coefficient differences, i.e., $p = q = i$, and the corresponding variances of the QL-GFA and the reference models, of the combined SST-SGG gravity field solution. Assuming a level of significance $\alpha = 0.05$, the critical value of the F-distribution is given by $F_{0.95}(1,\infty) = 3.84$. The upper limit of the colorbar in Fig. 7 (a) was chosen correspondingly. Fig. 7 (a) demonstrates that the coefficient estimates are more or less consistent with their corresponding error estimates. The largest test variables occur in the polar gap region, indicating that the MSE estimate (Fig. 5 d) is slightly too optimistic.

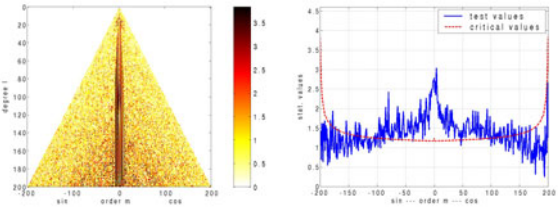

Fig. 7. Test statistics per coefficient T_{lm} (left) and per order T_m (right)

As discussed in section 5.4, in the ideal case all test variables T_{lm} should be below their critical values, i.e., the differences x should be strictly random. However,

several (smaller) error sources are non-stochastic and remain unmodelled, leading to a non-ideal white noise behaviour of the residuals, and correspondingly also of the coefficient estimates. The same picture is expressed by analyzing order-wise blocks of coefficients. The [blue] solid curve in Fig. 7 (b) shows the test variables T_m, and the [red] dashed curve the corresponding critical values.

A similar analysis (not shown) was done using independent gravity field models $x^{(0)}$, with non-vanishing covariance information $\Sigma(x^{(0)}) \neq 0$. In this case, the test statistics are considerable lower as in the very strict case shown in Fig. 7. Such types of analysis, together with the results of the hypothesis tests applied to the residuals, are summarized in the Quality Report Sheet, which is part of the product EGM_QLB_2i.

7. SUMMARY AND CONCLUSIONS

In this paper the architectural design of the Quick-Look Gravity Field Analysis software, as part of the Sub-Processing Facility 6000, is described. The software is now fully implemented, integrated and tested, and its status is operational. On the basis of the official HPF Acceptance Test scenario, the data flow and the output products have been described in detail. Due to the fact that the semi-analytic approach, underlying QL-GFA, is based on several simplifying assumptions, compared to an ultimate-precision solver the accuracy of the gravity field products is decreased by a factor 1.5 to 2. However, the main goal, i.e. to perform a check of the input data on the level of a gravity field solution, can be met by far.

8. ACKNOWLEDGEMENT

This study was performed in the framework of the ESA-project GOCE High-level Processing Facility (Main Contract No. 18308/04/NL/MM). It was supported by the Austrian Space Application Programme initiative by the FFG (contracts no. ASAP-CO-008/03 and ASAP-WV-211/05). Funding was also provided by the GOCE-GRAND project in the frame of the German "Geotechnologien Projekt".

9. REFERENCES

1. Badura, T., et al. Derivation of the CHAMP-only global gravity field model TUG-CHAMP04 applying the energy integral approach. *Stud. geophys. geod.*, 50, 59 – 74, 2006.

2. Földvary, L., et al. Gravity Model TUM-2Sp Based on the Energy Balance Approach and Kinematic CHAMP Orbits. In: Reigber et al. (eds.), *Earth Observation with CHAMP - Results from Three Years in Orbit*, 13-18, Springer Verlag, 2004.

3. Kern, M., et al. Outlier detection algorithms and their performance in GOCE gravity field processing. *J. Geod.*, 78, 509–519, 2005.

4. Koch, K.-R., and Kusche, J. Regularization of geopotential determination from satellite data by variance components. *J. Geod.*, 76, 259-268, 2002

5. Lackner, B. *Datainspection and Hypothesis Tests of very long Time Series applied to GOCE Satellite Gravity Gradiometry Data*. Dissertation, 187pp., Graz University of Technology, Graz, 2006.

6. Lemoine, F.G., et al. *The Development of the Joint NASA GSFC and the National Imagery and Mapping Agency (NIMA) Geopotential Model EGM96*. National Aeronautics and Space Administration, Goddard Space Flight Center, Greenbelt, Maryland, 1998.

7. Metzler, B., and Pail R. GOCE data processing: the Spherical Cap Regularization Approach. *Stud. Geophys. Geod.*, 49, 441-462, 2005.

8. Pail, R. A parametric study on the impact of satellite attitude errors on GOCE gravity field recovery. *J. Geod.*, 79, 231-241, 2005.

9. Pail, R., et al. *Quick-Look Gravity Field Analysis (QL-GFA)*. DAPC Graz, Phase Ia, Final Report, WP Ia-4.1, 107 - 161, Graz, 2003.

10. Pail, R., et al. GOCE gravity field analysis in the framework of HPF : operational software system and simulation results. *Proc. 3rd GOCE User Workshop*, Frascati, November 2006, European Space Agency, Noordwijk, 2006.

11. Pail, R., and Plank, G. Assessment of three numerical solution strategies for gravity field recovery from GOCE satellite gravity gradiometry implemented on a parallel platform. *J. Geod.*, 76, 462 – 474, 2002.

12. Pail, R., and Plank, G. GOCE Gravity Field Processing Strategy. *Stud. Geophys. Geod.*, 48, 289-308, 2004.

13. Pail, R., and Wermuth, M. GOCE SGG and SST quick-look gravity field analysis. *Advances in Geosciences*, 1, 5 – 9, 2003.

14. Preimesberger, T, and Pail R. GOCE quick-look gravity solution: application of the semianalytic approach in the case of data gaps and non-repeat orbits. *Studia geoph. et geod.*, 47, 435 – 453, 2003.

15. Rummel, R., et al. Spherical harmonic analysis of satellite gradiometry. *Neth. Geod. Comm., Publications on Geodesy*, 39, Delft, The Netherlands, 1993.

16. Rummel R, et al. High Level Processing Facility for GOCE: Products and Processing Strategy. *Proc. of the 2nd Internat. GOCE User Workshop*, Frascati, 2004.